https://doi.org/10.2352/ISSN.2169-4451.2017.32.194

Reprinted from
Journal of Imaging Science and Technology® 60(4): 040404-1–040404-9, 2016.

Multi Pulse Train Modeling of Piezo-Drop-on-Demand Inkjet Print-Head Response

Stephen D. Hoath▲
University of Cambridge, IfM, 17 Charles Babbage Road, Cambridge CB3 0FS, United Kingdom
E-mail: sdh35@cam.ac.uk

Abstract. *Resonant oscillations set up internal fluid waves within a piezo-drop-on-demand (DoD) print-head channel as a result of actuation drive pulses. Such waves will persist for some time after droplet ejection from the nozzle, and the residual wave amplitude can interfere (constructively or destructively) with all succeeding actuation drive pulses, potentially altering the speed and volume of successive droplets. As uncontrolled interference would worsen printing quality, residual waves are usually reduced by a combination of print-head design and waveform optimization for better performance at continuous (steady state) printing frequencies. However, the residual waves following any changes of printing frequency can influence "first" drops and short bursts of drops. Exact analytic expressions are provided here for the N-pulse burst DoD print-head response function with fixed printing frequency. This article explains the purpose and application of the model predictions to published piezo-driven DoD data. An examination of the effect of fluid properties, the identification of unexpected jetting behavior and some issues with manufacturing prototype quality, tests of assumptions made in the simple model and extensions to the prediction of print-head performance using realistic complex waveforms are also discussed. An earlier shorter article, mainly introducing the multi pulse train modeling approach and some applications within Xaar, was first presented at NIP31/DF2015 [S. D. Hoath, A simple model for DoD inkjet frequency response, Proc. IS&Ts 31st Int'l. Conf. on Digital Printing Technologies (IS&T, Springfield, VA 2015), 8–12].* © *2016 Society for Imaging Science and Technology.*

INTRODUCTION

As a result of the industrial marketing push toward ever higher inkjet printing (jetting) frequencies and smaller drop sizes, and the rapid progress being made in applications of micro-electro-mechanical systems (MEMSs)-based manufacturing, some drop-on-demand (DoD) inkjet print-head designs rely on piezo-actuated (driven) resonant chambers to generate liquid droplets. It is convenient to consider a single nozzle device, although the generalization to multiple nozzle print heads is both feasible and desirable. The resonant oscillations set up waves in fluid within each DoD print-head channel as a result of the actuation drive pulses.[1–3] Such waves will persist for some time in the channel after the droplet ejection from the nozzle,[4] and the residual wave amplitude can interfere (constructively or destructively) with all succeeding actuation drive pulses, potentially altering the speed and volume of successive droplets.[5] As uncontrolled interference would worsen printing quality, continuous printing residuals are often tamed by the combination of print-head design and waveform modifications.[6–9] Residual wave effects on the observed speed and volume of the last fluid droplet ejected by a short burst of (N) drive pulses, i.e., following distinct changes of printing frequency, and the steady state printing condition (where N is large) are also predicted using multi pulse train (MPT) modeling.[10] The effect of residual waves may also change the timing of the droplet, leading to drop misplacement, while incomplete refilling[11] or overfilling of the nozzle following droplet ejection can both have very major effects on the speed, direction and volume of the subsequent droplet(s) which are significantly harder to model than at lower printing frequencies without such complications for the initial conditions.

A simple approach to model the magnitudes of the (measurable) drop speed and volume from the print head treats the response for the last pulse of the N-burst as if it was generated with the phase and magnitude of an impulse peak response but then forms the resultant sum over damped residual waves after taking account of the actual phases and decay for all $(N-1)$ preceding impulses. This approach avoids nearly all of the details of the piezo-driven wave behavior during the waveform, while focussing on the implications for applications of DoD printing, which inherently involve both steady state (longer term) and transient (short term) bursts of pulses. For single isolated pulses, and a range of low frequencies for steady state printing, the residual waves will have diminished before another pulse is applied. Consequently, for such low frequencies, DoD print-head response can be considered as "normal." The residual wave oscillation amplitude immediately after an impulse equals the normalized value 1, and this amplitude diminishes exponentially with elapsed time to effectively reach zero before the start of any succeeding applied drive pulse. Clearly, for an extended pulse length, lack of sufficient residual wave damping would limit the maximum repetition rate (frequency) at which overlap of the residual wave oscillations from prior pulses and succeeding pulse(s) would interfere with the wave amplitude from the nth pulse. The relative phase of the damped residual waves and the succeeding pulses determines whether the overlap enhances their summation constructively or destructively. Indeed,

▲ IS&T Member.

Received Mar. 4, 2016; accepted for publication June 9, 2016; published online July 29, 2016. Associate Editor: Kye-Si Kwon.

extended pulse waveform designs for DoD inkjet print heads are often deliberately engineered to produce droplets of a specific speed and volume simultaneously with minimum possible absolute amplitude for the residual wave. This usually raises the maximum (steady state) printing frequency range within which some specific tolerances on the jetting characteristics of the droplets, for example the allowable variations in drop speed and volume, can be maintained. As will be shown, the flat bandwidth frequency range over which piezo-driven DoD drop speeds are kept within specifications of ±5% is closely linked to the overall damping factor (Q) of the print-head's (natural) resonance frequency (f_H), at least for applied drive waveforms comprising a single unipolar pulse.

More complicated waveform designs for specific combinations of piezo-driven DoD print heads and fluids often aim to extend the useable frequency range beyond its flat (unipolar pulse) bandwidth. Importantly, where the desired drop speed is relatively high, suitable control of the "pinch-off time" for a fluid jet may avoid unwanted "satellite" production, by sufficiently reducing the inkjet ligament length at the required jetting speed, and simultaneously enable successful higher frequency printing. There are other technical reasons for developing more complex drive waveforms, which are outside the scope of this article. Some, for example, grayscale printing, can be approached within the spirit of the present multi pulse train model, which will be described in some detail in a later article.

It must be emphasized that piezo-driven DoD print heads are usually driven by complex waveforms to achieve the best performance in applications. In this article a simple waveform is used so that underlying responses of the piezo-driven DoD print heads themselves can be better revealed. This aids in the identification of more fundamental performance limits and, following the application of linear response theory, in more easily investigating the potential directions for beating these limits.

RESIDUAL WAVE MODELS FOR BURST AND CONTINUOUS PRINTING

Earlier analytic work[2,3] on the residual wave responses for multiple coupled channels in piezo-driven DoD arrays focussed on results in the time domain, rather than in the frequency domain as herein. Recent use of advanced control theory[7–9,12] has now produced robust optimized DoD waveforms, a method that provides a direct route to a specific residual wave duration and frequency bandwidth.

To a certain extent, the present approach allows print-head characteristics to be inferred (reverse-engineered) from the measured frequency response for both the jetted droplet speed and volume. The exact analytic summations could easily be replaced (and extended) by numerical summations, which could then be used to construct and investigate more general DoD drive waveform tools. However, for the present explanatory purposes, only exact analytic results will be considered here. Furthermore, explicit results for burst, as well as continuous, printing are provided for the first time.

All approaches to exact modeling of residual waves in resonant piezo-driven DoD print heads rely on the linearity of the equations of motion in time, which implies that wave amplitudes (perhaps from different physical sources, or events such as the drive pulse) can be simply added together by taking into account their magnitude and relative phase.[3] After a particular drive pulse completes, an associated residual wave starts at time $t = 0$. The previous drive pulse would have been decaying away for time $t = 1/f$ at the fixed printing frequency f, and its amplitude would have decayed through the $\exp(-b/f)$ factor while the phase of the (cosine) oscillation would have altered by the angle a/f. This previous wave continues to decay, independently of the new wave, but after the particular drive pulse has finished, the overall residual wave amplitude will be the sum of these two independent waves. Thus, linearity suggests that the resulting residual wave after two pulses is $1 + \cos(a/f)\exp(-b/f)$ at frequency f, after three pulses is $1 + \cos(a/f)\exp(-b/f) + \cos(2a/f)\exp(-2b/f)$ and after N such pulses at this frequency equals $\sum[\cos(na/f)\exp(-nb/f)]$, where $\sum[]$ is the multi pulse train summation of the nth pulse over N pulse contributions, formed by n taking the successive integer values from 0 to $N - 1$.[10]

EQUATIONS

Evaluation of $\sum[]$ exploits the exact analytical result $(1 - z^N)/(1 - z)$ for complex number z, where $|z| < 1$, $\mathrm{Re}\{\exp(ja/f)\} = \cos(a/f)$ and $\mathrm{Im}\{\exp(\pm ja/f)\} = \pm\sin(a/f)$ $j = \sqrt{(-1)}$, and identifying $\sum[z^n]$ with the real part $\mathrm{Re}\{\sum[z^n]\}$. By replacement of $\cos(a/f)\exp(-b/f)$ by $z = \exp(-b/f + ja/f)$, and noting $z^* = \exp(-b/f - ja/f)$, we find that $Re\{\sum[z^N]\} = Re\{(1 - z^N)/(1 - z)\} = [Re\{(1 - z^N)(1 - z^*)\}]/[(1 - z)(1 - z^*)] = [Re\{1 - z^* - z^N + z^N z^*\}]/[1 - z - z^* - z^* z]$, and so we find that $\sum[] = R(N, f) = [1 - \cos(a/f)\exp(-b/f) - \cos(Na/f)\exp(-Nb/f) + \cos(a(N - 1)/f)\exp(-(N + 1)b/f)]/D(f)$, where $D(f) = [1 + \exp(-2b/f) - 2\cos(a/f)\exp(-b/f)]$. In the steady state limit $R(N, f) \Rightarrow R(f) = [1 - \cos(a/f)\exp(-b/f)/D(f)]$. The rather useful finding that the denominator $D(f)$ is independent of N simplifies both $R(N, f)$ and $R(f)$. We find that this steady state result $R(f)$ follows immediately from properties of the Z-transform.[13] (Furthermore, the properties of the Z-transform can be used for evaluating summations over terms involving $\sin(na/f)\exp(-nb/f)$ as easily as those in $\cos(na/f)\exp(-nb/f)$ within the summations for $R(f)$.)

CHARACTERIZATION OF RESIDUAL WAVES IN FLUID JETTED BY A PIEZO-DRIVEN DOD PRINT HEAD

For a damped oscillatory wave that has a normal amplitude, the simple function $\cos(at)\exp(-bt)$, takes the value 1 at elapsed time $t = 0$ and then oscillates at a frequency $f_D = a/2\pi$ and decays at the rate $b = \pi f_H/Q$, where a and b are considered to be constants. The quality factor Q for

resonant DoD inkjet print heads links the damped frequency f_D and natural frequency f_H through relationships[14] such as $f_D = f_H\sqrt{\{1 - 1/(2Q)^2\}}$ for a single degree oscillator, where usually $Q \gg 1/2$. This latter case[14] implies that $b \approx a/(2Q)$ for all of the dominant and higher-order residual waves in inkjet print heads. We avoid choice of the oscillator model and approximating the rate of damping (b) in our derivations so that other highly (but still resonant) damped residual waves can also be included in the frequency response.

CONSEQUENCES OF *Q*-FACTORS FOR INKJET PRINT HEADS

Resonant inkjet print heads excited with constant voltage unipolar pulses can have high frequency responses that show jetted drops with far higher or somewhat lower speeds than at low frequency, to an extent that depends on the Q-factor and the (dimensionless) printing frequency ratio f/f_H. Starting at low printing frequencies, if the response is normalized to unity, then for response peaks (highs) occurring at higher frequencies due to constructive residual oscillations, the (voltage) level(s) of the (unipolar) actuation pulse used to drive the piezo-DoD print head could be reduced in order to compensate this, with potential benefits to the device power consumption and lifetime. Conversely, wherever the printing frequency produces a normalized response below unity, e.g., near valleys (lows) of destructive residual oscillations, the level(s) would need to be increased for compensation, with higher device power and cooling requirements and limiting fluid viscosity. Other scenarios are possible for compensation: the pulse waveform duration or its level of complexity could be altered. Print-head operation near frequencies corresponding to peaks (or valleys) of the print-head system response can still be distinctly advantageous for some applications requiring highly stable response. However, further mention of choosing an operating frequency lies beyond the scope of this article.

VISCOUS FLUIDS AND INKJET PRINT-HEAD *Q*-FACTORS

The multi pulse and steady state printing frequency responses derived exactly for simple piezo-drive pulses in an earlier section can be interpreted in terms of the frequency f_H and damping Q-factor of the print head and fluid combination. The chosen material and mechanical properties, the design and the physical build of the print head might be expected to dominate the natural resonant frequency, while the damping also depends on the relevant properties of the fluid (such as density and viscosity). Non-Newtonian fluid behavior, density, compressibility (including effects due to dissolved gases), elasticity and dynamic surface tension may alter the apparent natural frequency of the resonance, as could inclusion of material components with extra compliance (or arising from defective bonds). Mechanical, fluidic or electrical cross-talk present between neighboring channels would also be expected to influence the apparent damping factors dependent on which nozzles were being driven, and with what drive and phase. Such considerations are avoided in the present work, as they are better included within numerical simulations more easily than in analytic forms.

Fluid properties, such as the speed of sound, significantly control the values of Q and f_D, but it is also worthwhile to explain how some additional losses might change Q-factors for print heads. Such additional losses may be (unintended) consequences of changing the jetted fluid viscosity, e.g., while successively setting up and using different fluids or operating temperatures with a print head.

It should be recalled that Q-factors are a measure of stored energy ÷ power lost over an oscillation period. It can be noticed that constant $b = \pi f_H/Q$ involves reciprocal $1/Q$, thus proportional to total power lost ÷ stored energy. Therefore, $1/Q$ = (head loss + fluid loss) ÷ storage = head loss ÷ storage + fluid loss ÷ storage = $1/Q_0 + 1/Q_V$, where $1/Q_0$ represents the head contribution and $1/Q_V$ the (viscous) fluid contribution to total $1/Q$. Fluid losses thus increase $1/Q_V$ from 0 for inviscid fluids to higher values linearly with finite viscosity.

The two (possibly simultaneous) physical contributions to the decay constant b are the magnitude of the resonant frequency, f_D, and the magnitude of the total losses (including the fluid viscosity). While f_D depends on mechanical compliances for a given print-head (resonance chamber) geometry, the most obvious fluidic influence on f_D arises from the speed of sound corrected for compliance of the environment.[15,16] For printer and fluid combinations with the same speed of sound and f_D values, comparison of the observed values of the residual wave damping rate (b) found for fluids with different but known viscosities could be used to infer the values of $1/Q_0$ and $1/Q_V$ for each fluid jetted, and even to predict the effective Q-factor for other fluids to be jetted by that particular inkjet print head. One may anticipate that more viscous fluids may have lower Q and more highly damped responses in inkjet print heads, but direct measurements of residual waves could confirm or reject such changes. Importantly, frequency sweeps conducted for different fluids in the same print head could differ in a predictable fashion (higher viscosity should lead to lower Q and more damped frequency responses).

RESULTS

An application of the MPT model has been made to data shown in Figure 3 of Derby and Reis (2003) replotted here as Figure 1, for jetting paraffin with 0, 20 vol% and 40 vol% alumina powder loadings.[15,16] Note that the drop volumes for this particular example are typically ten to a hundred times larger than for recent SiMEMS print heads.

The overall reduction in drop volume, as particle loading is increased, arises from a combination of the fixed drive voltage applied to the print head and the increasing viscosity of the fluid with loading. In the present application of the MPT model, this difference between fluids is lost to normalization by each fluid's low frequency volumes (for which residual waves fully decay between printing drops).

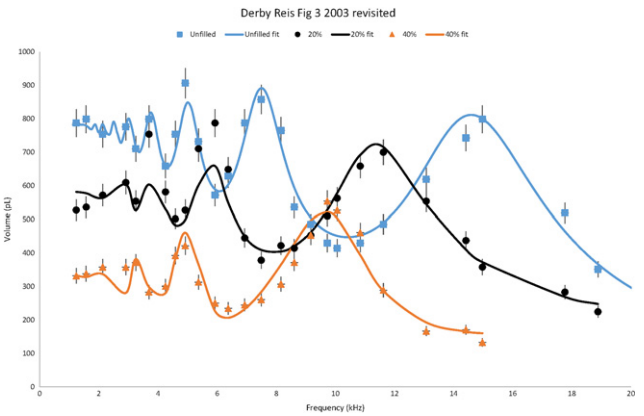

Figure 1. Measured drop volume, as a function of DoD printing frequency, for liquid paraffin loaded with alumina powder[15,16] as compared in a self-consistent analysis with $R(f)$ from the MPT model for the unloaded paraffin response. The fitted f_D and Q values vary with the speed of sound in these fluids. See text.

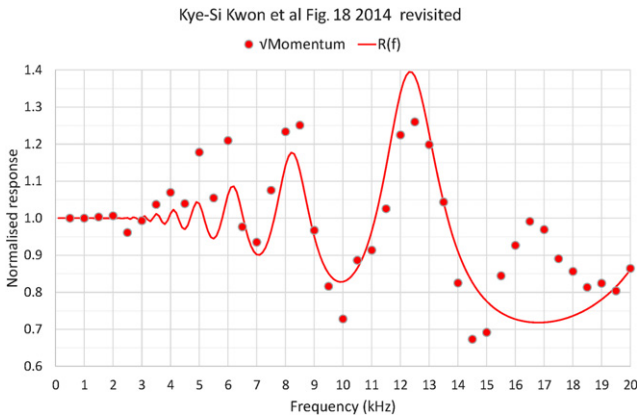

Figure 2. Published data[17] shown as normalized $\sqrt{}$(speed×volume) are compared with $R(f)$. See text.

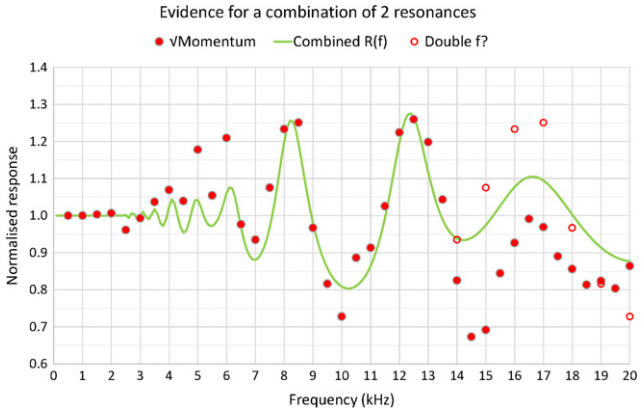

Figure 3. Published data[17] as in Fig. 2 but with superposed fictional data (shown as unfilled symbols) at double true frequency (Double f) compared with a combined weighted response from two independent resonances. See text.

Exact model frequency responses computed between 1 and 20 kHz were overlaid and manually fitted to the data trends by suitable adjustments of the Q-factors and damped frequencies assumed during printing.

Fig. 1 shows that at each loading the highest frequency peak F is the main ($m = 1$) resonance, as can most easily be seen by tracking the sub-harmonic ($m = 2, 3, 4, \ldots$) frequencies (F/m) for the unloaded 0 vol% data. The lowered print-head resonant frequency F as particle loading is increased agrees reasonably with the reduction in the speed of sound within the print head also computed by Derby and Reis.[15,16] Ignoring background slopes, the MPT model fits to each fluid's normalized data, assuming that the Q-factor as a free parameter can reasonably approximate the large % variations seen in 0.1–0.9 nano-liter scale droplet volumes. The fits show that the physical properties of the jetted inks, differing significantly between material loadings, had a major influence on the effective (damped) Q-factors, thereby distorting the frequency response spectrum. As the %volume loading increases, the fitted Q-factors are 6.8, 5.5 and 4.5. As $Q = 2\pi f_H \times$ stored energy $\div$ power loss, the speed of sound in a (loaded) fluid influences both the damped frequency (f_D) and the quality factor (Q) of the print head in the same (linear) manner. As the predicted change of the speed of sound with %volume loading, and hence the change of the damped frequency f_D, compared almost directly with the trends in Q-factors fitted to the corresponding jetting data,[15,16] no changes to the Q-factors could be ascribed to the effects of the greatly increased viscosity as the %volume loading was increased, meaning that viscosity only influenced the drop volume because a constant drive voltage was used with this particular print head.

In Figure 2, measurements for inkjet drop jetting published as normalized values of drop speed and drop volume[17] have been combined as normalized $\sqrt{}$(speed × volume) for comparison to predicted $R(f)$ from the simple MPT model, assuming a natural resonance frequency near 24.8 kHz and a Q-factor of about 5. (It should be noted that the term $\sqrt{}$(speed × volume) is proportional to $\sqrt{}$(momentum) for fixed drop density. For this particular experiment the absolute values of drop speed and volume could not be disclosed, while a physical model suggested that drop momentum would prove to be more representative.) The failure of this $R(f)$ to predict the presence of a ∼16.5 kHz response peak, despite good correspondence with the lower sub-harmonic peak locations at 12.4, 8.4, 6.2, 4.9 kHz. . ., their relative strengths and even the "flat-background" limit $B = 4.9$ kHz could point to the presence of additional resonances in the inkjet print head, such as the presence of a refill mode in this device[17] or a meniscus oscillation mode.

An example chosen to mimic the possible location of another independent resonance mode, which may represent refill but fails to properly represent the loss of drop volume that is inherent in refill, is shown in Figure 3 for the same data as used in Fig. 2. Nevertheless, some features of the resultant weighted frequency response do appear to represent the data quite well, by assuming somewhat arbitrary choices for the relative strength, natural resonant frequency and Q-factor to

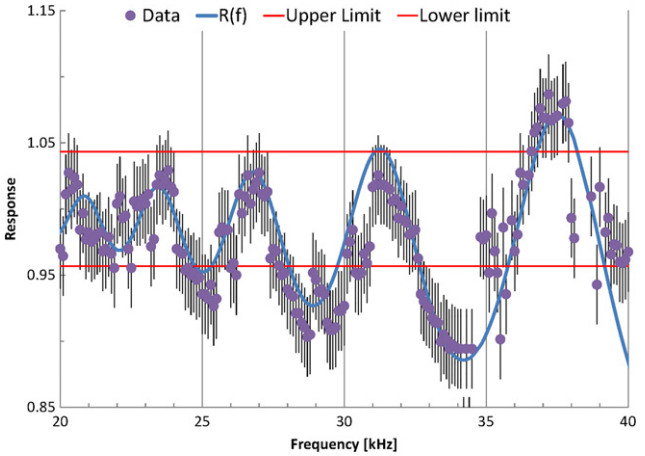

Figure 4. Measurements of drop speed for a XJ1001 print head at 20–40 kHz printing frequencies with the fitted $R(f)$, upper and lower limits superposed.[10]

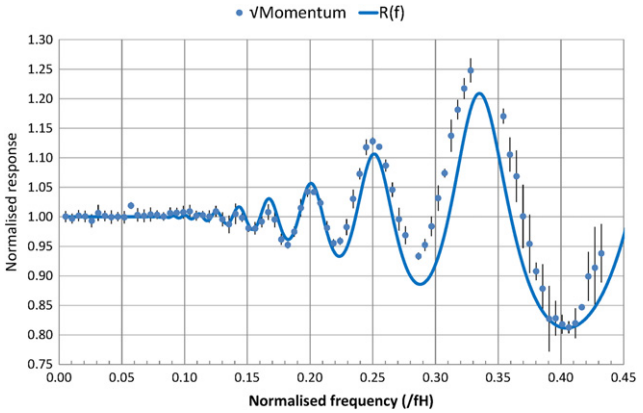

Figure 5. Measured drop speed and volume data for a particular SiMEMS DoD product development print-head geometry for a wide range of printing frequencies are combined as √ (momentum) and compared with the response $R(f)$ of the MPT model. These data are normalized along both axes.[10]

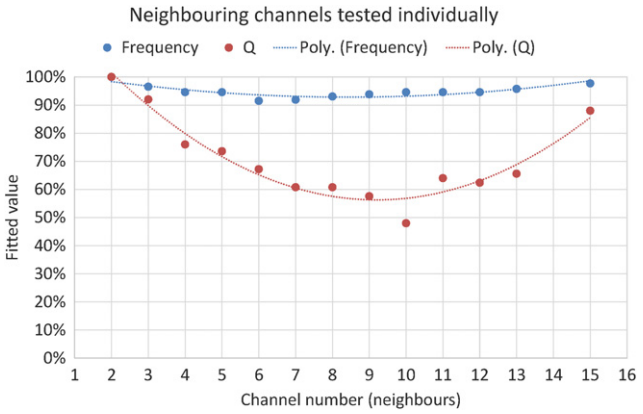

Figure 6. Results obtained by fitting the MPT model predictions to the single jetting channel drop speed frequency sweeps, for a bank of neighboring channels in a development prototype Si-MEMS device that contained known device bonding faults toward the center of the array. The curves merely guide the eye and clearly have no intrinsic meaning between channel numbers. The parameters f_H and Q have been normalized to fitted channel 2 values and interpreted in the text.

achieve this. The (unpalatable) alternatives are a complete failure of the simple MPT approach, or high frequency measurement issues for imaging software or even some neglected physics relevant to inkjet printing. As a merely empirical (and hopefully unconvincing) gesture toward an alternative, some of the data in Fig. 2 has been replotted on Fig. 3 at twice their correct frequencies for a comparison with the apparent location and width of the additional resonance, as they do roughly correspond.

To challenge the MPT modeling approach seriously, high frequency jetting data will be examined next. Figure 4 shows drop speeds at fixed 20–40 kHz jetting frequency, from an independent laboratory, for a standard XJ1001 print head.[10] $R(f)$ is shown in blue on an arbitrary cubic background variation, while the data were normalized for comparison purposes to the average drop speed between 5 kHz and 6 kHz. The normalized speed range specified by $1 \pm \exp(-\pi) = 100 \pm 4.32\%$ is also superposed on the graph. (Note that for applications the print head would not normally be driven by the same simple drive waveform as used to generate the response shown here.)

Figure 5 shows some product development data on DoD drop speed and volume measurements for a certain print-head geometry converted into normalized √ (momenta) versus normalized frequency (i.e., kHz/f_H) for consistency with the NIP31/DF2015 conference article.[10] The error bars reflect the spread of results for 10 drops measured (using a JetXpert^{TM}) at each steady state printing frequency. The comparison between the shape and magnitude of the frequency sweep data and the MPT model prediction $R(f)$, which is here shown without an underlying "background", illustrates the quality of both the data (being the harmonic mean of the drop speed and drop speed) and the model. The benchmark provided by such modeling assisted with the early elimination of production issues.

A final example of the application of the MPT model predictions returns, in a sense, to the impact of losses on Q and hence the shape of the frequency sweeps. Figure 6 shows normalized results from fitting the two free parameters (f_H and Q) of $R(f)$ to frequency sweep (speed) data measured for a bank of individually actuated next-neighbor channels in a development prototype device that contained known device bonding faults toward the center of the array. Unlike the previous case considering losses, the same fluid was jetted from each channel, and the variations of Q are much larger than those of the resonance. The implication was the presence of other sources of losses for individual channels. Subsequent IR camera inspection revealed an issue with unwanted leakage between channels that corresponded to trends shown in the fitted Q-factor. Such early successes underpinned the value of the MPT approach for benchmarking DoD response, and improved the automated assessment of jetting data sets across development design devices. For some print-head designs it is reasonable to talk about the Helmholtz frequency

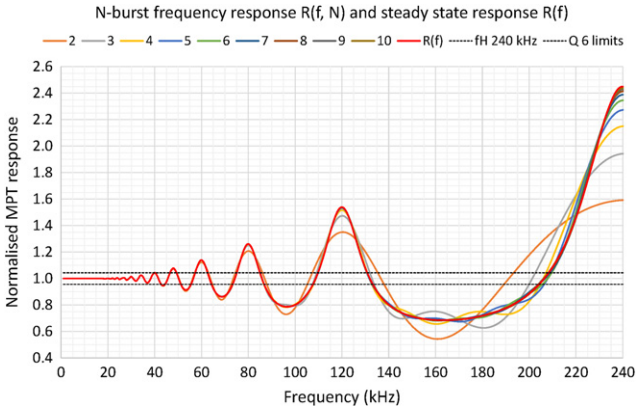

Figure 7. The N-burst frequency (f) response $R(f, N)$ and steady state response $R(f)$ resulting from a single exponentially damped cosine oscillator having natural resonance $f_H = 240$ kHz and Q-factor 6. These representative values lead to sub-harmonic peaks at conveniently located frequency values for steady state printing. The flat-background frequency region defined by $f < B = f_H/Q$ ($= 40$ kHz here) corresponds to the upper and lower (dashed line) limits at $1 \pm \exp(-\pi) \approx 100\% \pm 4.3\%$ that just "touch" the Qth sub-harmonic peak of $R(f)$. Approaching the steady state printing response, $R(f)$ requires bursts of $N > Q$ pulses.

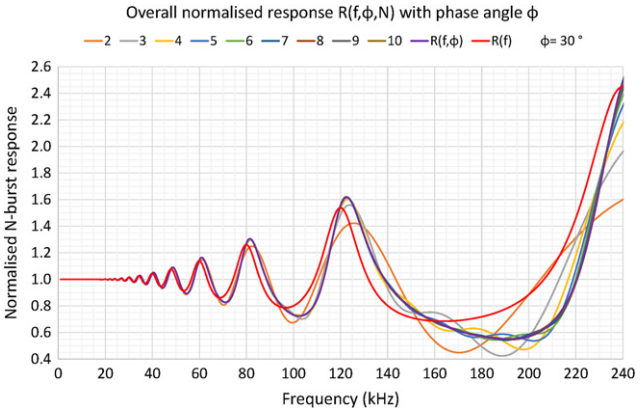

Figure 8. Overall normalized response $R(f, \phi, N)$ compared with the steady state response $R(f, \phi)$ for a phase angle $\phi = 30°$ and the steady state response $R(f)$ with $\phi = 0°$, for $f_H = 240$ kHz and $Q = 6$. See text.

(f_H), while for others it is reasonable to talk about the wave speed and associated modes, but this does not detract from MPT summation of residual waves.

COMPLICATED DRIVE WAVEFORMS

Generalization of this MPT approach to predict the effect of complicated drive waveforms is quite straightforward (if unwieldy): just add suitably weighted and phased combinations of the linear response $R(f)$ found for unipolar excitation of the print head and fluid used. For example, the explicit exact summations for the extra time dependences of residual wave generation by ramped unipolar waveforms, as given previously,[3] can be immediately handled using the MPT method for complex z. The properties of the Z-transform[13] can be applied to finite sums over decaying sine waves, and give the same denominator $D(f)$ as was found for the sums over decaying cosine waves resulting in $R(f)$. Thus, decaying waves of any phase are handled by decomposition into cosine and sine components. Additional drive pulses with appropriate weights and phases can be used to represent bipolar and grayscale printing waveforms. Numerically summing $R(f)$ terms, rather than exact results, has been proposed, so the exact mathematical results for such extensions of the simple MPT model are not given here.

BURST PRINTING

The majority of inkjet printing applications also involve short bursts of printing (N) drops rather than steady state printing, and it was shown earlier[10] that the simple MPT model can easily provide exact predictions for the evolution of the N-burst frequency response $R(f, N)$ with increasing N toward the steady state response $R(f)$ that might be expected for a given print head characterized by f_H and Q. It should be noted that the printing frequency response curve for a single drop (i.e., $N = 1$) does not physically exist, although the purely mathematical representation would be a straight line $R(f, 1) = 1$ at all frequencies, reflecting the normalization for the MPT model. The achievement of near steady state requires $N > Q$ pulses.

Figure 7 shows the N-burst frequency response $R(f, N)$ for $N = 2$–10 and also the steady state response $R(f)$, together with the upper and lower limits, for the case $f_H = 240$ kHz and $Q = 6$. Figure 8 shows the evolution for the N-burst frequency response $R(f, \phi, N)$ compared with the steady state response $R(f, \phi)$ for phase angle $\phi = 30$ degrees and the steady state response $R(f)$ with $\phi = 0$ degrees, for $fH = 240$ kHz and $Q = 6$. In both figures the major changes are, as expected, between $N = 2$ and $N = 3$, persisting to $N > 6$ for high frequencies. The steady state MPT response appears to hold after $N > Q$ pulses (with same drive) at the same frequency.

DISCUSSION

Changes predicted by the simple MPT model, between the earliest drops of N-burst printing and later continuously printed drops in steady state printing, are considered as "first drop" effects completely unrelated to the evaporation of ink,[18] raised concentrations of particles at the DoD nozzle meniscus, which are often associated with (extended) non-printing periods,[19] rather low printing frequencies,[20] or even unmerged satellites (which have been detected using holographic methods).[21] Although the MPT model predictions are inherent to DoD inkjet printing, they could be completely masked or distorted by conditions for fluid jetting and the complicated drive waveforms intended to reduce the effect of residual oscillations on steady state printing. Although response changes are completely predictable for N-burst printing, using any waveform, there has not been previous mention of their existence in the inkjet printing literature.

In contrast to this, the phase angle to represent the release time of a drop within the cycle relevant to the excitation of a wave response in DoD printing has been

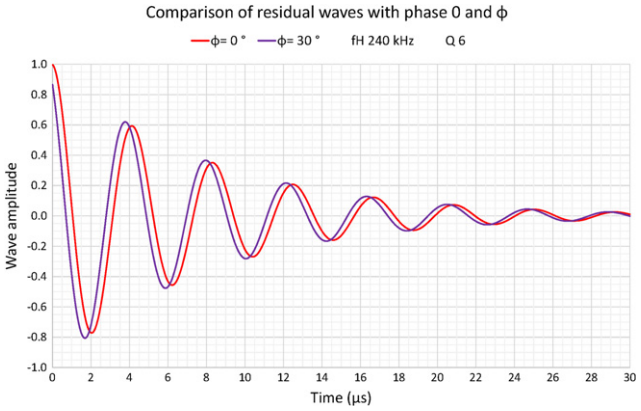

Figure 9. Comparison of the time evolution of residual waves for phase $\phi = 0°$ and $\phi = 30°$, for $f_H = 240$ kHz and $Q = 6$.

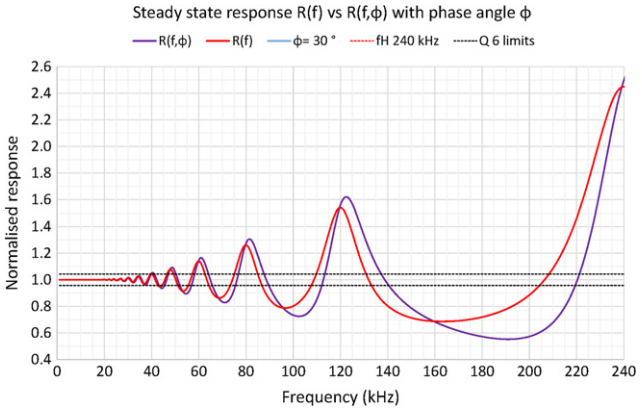

Figure 10. Comparison of the steady state printing responses $R(f, \phi)$ and $R(f)$, where phase $\phi = 30°$, for $f_H = 240$ kHz and $Q = 6$. See text.

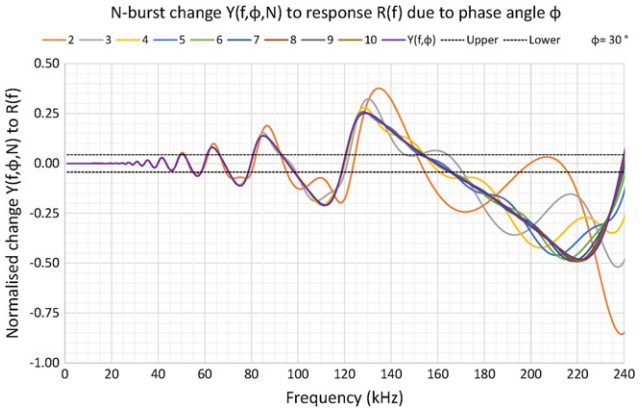

Figure 11. The shape of the correction $Y(f, \phi, N)$ after N-burst printing ($N = 2$–10) and phase $\phi = 30°$, for $f_H = 240$ kHz and $Q = 6$. See text.

analyzed in some detail previously.[3] In the $(\omega_0 t^*)$ phase nomenclature of Dijksman and Pierik,[3] for sine waves rather than the cosine waves of the present work, the release for drop jetting speeds above thresholds imposed by the surface tension was stated to be $(\omega_0 t^*) = 2\pi/3$. This should be equivalent to $\phi = (\omega_0 t^*) - \pi/2 = \pi/6 = 30°$. The worst case scenario envisaged is that the phase angle only applies to the timing of the response on the cosine wave but NOT on the exponential damping. Slightly weaker effects arise if the phase applies to the cosine wave AND the exponential damping term. (Both are considered in the appendix.) Comparisons with real response data showed only minor effects from these different phase angles.

Figure 9 shows the time evolution of residual waves for zero phase and for this finite phase ϕ value, and Figure 10 shows the impact of either choice on the steady state printing response, $R(f)$ and $R(f, \phi)$, respectively. The differences between these cases are primarily shifts toward (a) higher frequency sub-harmonic peaks, (b) larger swings and (c) higher asymmetry around these frequency peaks, and in particular steeper inclines and more gradual falls as the frequency is swept over all of these peaks. The similarities are mainly in the flat-background region, which for $\phi = 0°$ was <40 kHz, although a finite phase angle $\phi = 30°$ has slightly reduced the flat-background region due to (b) and (c) above.

Figure 11 confirms that the shape of the correction $Y(f, \phi, N)$ to the steady state printing response $R(f)$ rapidly approaches the steady state correction shape $Y(f, \phi)$, arising from the finite phase angle $\phi = 30°$, and the number of pulses N increases from 2 to 10. In Figs. 10–11, showing frequency sweeps as a function of N, the single pulse ($N = 1$) response is omitted because there can be NO frequency spectrum without a repetition!

CONCLUSIONS

Multi pulse train (MPT) model predictions for burst and steady state piezo-DoD inkjet printing at a fixed frequency are given in both cases by exact but quite straightforward analytical results assuming impulse responses for each pulse and linear summation of wave amplitudes. Extensions of the MPT model results to far more complex waveforms, such as those commonly used for such DoD print heads, involve the combination of further but similar terms and (as usual) taking into account their relative phase.

Some key assumptions underlying the use of a simple impulse response for the MPT model have been examined by comparison with other published model approaches to computing residual wave amplitudes and phases. In particular, phase angle effects cause a frequency-dependent modification of the MPT model which only appears for higher frequency jetting, and appears to be quite small provided that the drop speed is well above the threshold for droplet production.

Drop measurement data for steady state printing, recorded over a range of frequencies by research teams using different types of resonant piezo-DoD print heads driven by simple unipolar waveforms, are well described by the MPT model with just two adjustable parameters: the natural frequency and the quality factor.

Changes (in jetted droplet speed and volume) between the first (few) drop(s) and later continuously printed drops appear in the MPT model as a "first drop" effect unrelated to the evaporation of ink or other effects on the fluid in or on the resting meniscus at the nozzle exit immediately beforehand.

Self-consistent data analyses using the MPT model showed that loaded fluid properties can alter DoD printing frequency spectra, by reducing the effective resonant frequency and Q, although additional effects on Q arising from significant viscosity changes were not detected. The direct application of the simple MPT model response for a unipolar "push" waveform driving a resonant piezo-DoD inkjet print head to jet particle loaded fluids gave a quantitative understanding of the jetting data.[15,16]

An additional (unexpected?) resonant response in a measured frequency sweep[17] was identified by linearly combining the MPT model predictions for the major peaks with an independent MPT model term for the additional response, thus enabling this to be characterized for future research studies.

Higher frequency jetting response data[10] obtained using simple waveforms were also fitted by MPT model predictions. The results of comparisons between different piezo-DoD inkjet print heads can also assist with future product design, formulation of waveforms for improved performance (drop speed, drop volume and frequency range) and indications of jetting sensitivity to fluid properties.

ACKNOWLEDGMENTS

This work was supported by an EPSRC Impact Acceleration Knowledge Transfer Fellowship (Grant no. EP/K503757/1) and industrial funds from the Inkjet Research Centre at the University of Cambridge. Xaar and other consortium members within the I4T (innovation in industrial inkjet technology) project (Grant no. EP/H018913/1) gave permission to publish earlier results in NIP31/DF2015 and also provided further support. Graham Martin (University of Cambridge), Mario Massucci, Tony Cruz-Uribe and Marko Dorrestijn (Xaar Cambridge), and Eva Singler and Ingo Reinhold (Xaar Sweden) all shared their unpublished piezo-DoD print-head data, comments and suggestions for this article. Helpful comments from the JIST reviewers are also gratefully acknowledged.

APPENDIX

The MPT response $R(f,\phi,N)$ that corresponds to residual waves out of phase by the angle ϕ (which may itself be a function of the frequency f) requires an evaluation of $\sum[\cos(\phi+an/f)\exp(-bn/f)]$ over the usual range of n from 0 to $N-1$. For reasons of space, the full derivation for the steady state printing response $R(f,\phi)$ is shown, whereas the final result for the burst printing response $R(f,\phi,N)$ is quoted.

As before, we substitute for the n-pulse term $z^n=\exp(-nb/f+jna/f)$ getting complex $\sum z^n=1/(1-z)$, but then combine $(1-z^*)$ and the complex multiplier $\exp(j\phi)$ accounting for the phase angle, before taking the real part and dividing the result by $D(f)$ and $\cos(\phi)$ to find $R(f,\phi)$. This result is phase-shifted from the usual $R(f)$ since $R(f,\phi)=R(f)\{1-\tan(\phi)\exp(-b/f)\sin(a/f)/[1-\exp(-b/f)\cos(a/f)]\}$ equals $R(f)$ only when $\phi=\pi m(m=0,1\ldots)$. Phase angles given by $\phi=(m+1/2)\pi$ for $m=0,1\ldots$ are unphysical because they correspond to adding up residual waves of zero magnitude (since $\exp(-bt)\sin(at)=0$ at $t=0$) following each pulse. Such waves are irrelevant anyway, because the observed DoD inkjet response (drop momentum, speed and volume) is well modeled by others[3] to correspond with a phase $|\phi|<\pi/2$.

The N-pulse burst frequency spectrum is found similarly by forming $R(f,\phi,N)=R(f)+Y(f,\phi,N)$, with $Y(f,\phi,N)=-(\tan(\phi)e^{-b}\sin(a)+e^{-Nb}\{\cos(Na)-e^{-b}\cos((N-1)a)-\tan(\phi)[\sin(Na)-e^{-b}\sin((N-1)a)]\})/D(f)$, and where the a and b variables in the function arguments actually represent a/f and b/f, respectively.

The damping term $e^{-Nb}\{\}$ within $Y(f,\phi,N)$ for $f<$ "flat bandwidth frequency" reduces below $e^{-\pi}=4.32\%$ as N increases above ca. Q pulses, irrespective of the phase angle $(0\le\phi<\pi/2)$. However, any non-zero ϕ introduces additional frequency distortions to the simplest form $R(f)$, derived assuming phase $\phi=0$, even in the limit of steady state printing, through an additional oscillating term $\tan(\phi)e^{-b}\sin(a)/D(f)$.

The phase angle ϕ can be ANY function of frequency, but provided that ϕ remains constant during a particular printing burst, the general result $R(f,\phi,N)$ will hold. Since this should also remain true for steady state printing, predicted frequency sweep shapes can be compared with the observed response to deduce changes of phase angle as a function of frequency.

Print bursts of int(Q) drops below the flat bandwidth frequency are sufficient to approach the simplest form $R(f)=\{1-\exp(-b/f)\cos(a/f)\}/D(f)$ for the DoD frequency response first presented at NIP31.[10] Ignoring the phase angle ϕ also leads to the N-burst frequency response derived before. This N-burst response can be expressed in the form $R(f,N)=R(f)\{1-\exp(-NB/f)(\cos(Na)-e^{-b}\cos((N-1)a))\}$ for zero phase shift.

REFERENCES

[1] T. Bogy and F. Talke, "Experimental and theoretical study of wave propagation phenomena in drop-on-demand ink jet devices," IBM J. Res. Dev. **28**, 314–321 (1984).

[2] J. F. Dijksman, "Hydrodynamics of small tubular pumps," J. Fluid Mech. **139**, 173–191 (1984).

[3] J. F. Dijksman and A. Pierik, *Inkjet Printing Technology for Digital Fabrication* (Wiley, 2013), pp. 57–66, chapter 3.

[4] J. R. Castrejón-Pita, S. D. Hoath, A. A. Castrejón-Pita, N. F. Morrison, and I. M. Hutchings, "Time-resolved particle imaging velocimetry within the nozzle of a drop-on-demand print-head," J. Imaging Sci. Technol. **56**, 1–6 (2012).

[5] M.-J. van der Meulen, H. Reinten, F. Dijksman, D. Lohse, and M. Versluis, "Experimental methods for retrieving flow information from within inkjet nozzles," J. Imaging Sci. Technol. **61** (2016).

[6] H. Wijshoff, "The dynamics of the piezo inkjet print-head operation," Phys. Rep. **491**, 77–177 (2010).

[7] A. Khalate, X. Bombois, R. Babuška, H. Wijshoff, and R. Waarsing, "Performance improvement of a drop-on-demand inkjet print-head using an optimization-based feedforward control method," Control Eng. Pract. **19**, 771–781 (2011).

[8] A. Khalate, X. Bombois, G. Scorletti, R. Babuška, S. Koekebakker, and W. de Zeeuw, "A waveform design method for a piezo inkjet print-head

based on robust feedforward control," IEE J. Microelectromech. Syst. **99**, 1–10 (2012).
[9] N. Morita, A. Khalate, A. van der Buul, and H. Wijshoff, in *Fundamentals of Inkjet Printing: The Science of Inkjet and Droplets*, edited by S. D. Hoath (Wiley-VCH, 2016), chapter 3.
[10] S. D. Hoath, "A simple model for DoD inkjet frequency response," *Proc. IS&T's 31st Int'l. Conf. on Digital Printing Technologies* (IS&T, Springfield, VA, 2015), pp. 8–12.
[11] J. F. Dijksman, P. C. Duineveld, M. J. J. Hack, A. Pierik, J. Rensen, J. E. Rubingh, I. Schram, and M. M. Vernhout, "Precision inkjet printing of polymer light emitting displays," J. Mater. Chem. **17**, 511–522 (2007).
[12] A. Khalate, X. Bombois, G. Scorletti, R. Babuška, S. Koekebakker, and W. de Zeeuw, "A waveform design method for a piezo inkjet print-head based on robust feedforward control," J. Microelectromech., Syst. **21**, 1365–1374 (2012).
[13] J. R. Ragazzini and L. A. Zadeh, "The analysis of sampled-data systems," Trans. Am. Inst. Elec. Eng. **71**, 225–234 (1952).
[14] University of Cambridge, Department of Engineering, Mechanics Data Book 2000, pp 6–12; 4.6 Harmonic response of a linear second-order system 4.6.3 case (c).
[15] B. Derby and N. Reis, "Inkjet printing of highly loaded particulate suspensions," MRS Bull. **28**, 815–818 (2003).
[16] C. Ainsley, N. Reis, and B. Derby, "Freeform fabrication by controlled droplet deposition of powder filled melts," J. Mater. Sci. **37**, 3155–3161 (2002).
[17] K.-S. Kwon, M.-H. Jang, H. Y. Park, and H.-S. Ko, "An inkjet vision measurement technique for high-frequency jetting," Rev. Sci. Instrum. **85**, 065101 (2014) Figure 18.
[18] A. Famili, S. A. Palkar, and W. J. Baldy, "First drop dissimilarity in drop-on-demand inkjet devices," Phys. Fluids **23**, 012109 (2011).
[19] K.-S. Kwon, H.-S. Kim, and M. Choi, "Measurement of inkjet first-drop behavior using a high-speed camera," Rev. Sci. Instrum. **87**, 035101 (2016).
[20] H. Dong, W. W. Carr, and J. W. Morris, "Visualization of drop-on-demand inkjet: drop formation and deposition," Rev. Sci. Instrum. **77**, 085101 (2006).
[21] K.-S. Kwon, L. Yang, G. D. Martin, R. Castrejón-Garcia, A. A. Castrejón-Pita, and J. Rafael Castrejón-Pita, in *Fundamentals of Inkjet Printing: The Science of Inkjet and Droplets*, edited by S. D. Hoath (Wiley-VCH, Weinheim, 2016), pp. 320–325, chapter 12.